BINDURA UNIVERSITY OF SCIENCE EDUCATION

FACULTY OF SCIENCE AND ENGINEERING

DEPARTMENT OF CHEMISRTY

THE ADSORPTIVE REMOVAL OF LEAD (II) IONS FROM AQUEOUS SOLUTIONS USING SUNFLOWER SEED HUSKS ACTIVATED CARBON / $CoFe_2O_4$ COMPOSITE

BY

MUNOTIDAISHE MHISHI

B213814B

SUPERVISOR: Dr. N. MUCHANYEREYI

A DISSERTATION SUBMITTED IN PARTIAL FULFILMENT OF THE REQUIREMENTS OF THE BACHELOR OF SCIENCE HONOURS DEGREE IN

CHEMICAL TECHNOLOGY (HBScCHT)

JUNE 2025

APPROVAL FORM

The undersigned certify that they have supervised, read and recommend to the Bindura University of Science Education for the acceptance of a research dissertation entitled:

The adsorptive removal of Lead (II) ions from aqueous solutions using sunflower seed husks activated carbon / $CoFe_2O_4$ composite.

Submitted by Munotidaishe Mhishi

In the partial fulfilment of the requirements for the Bachelor of Science Education Honors Degree in Chemical Technology

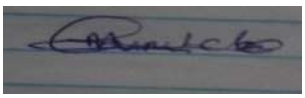

30/06/2025

(Signature of student) Date

30/06/2025

(Signature of Supervisor) Date

DECLARATION FORM

I, Munotidaishe Mhishi, do hereby declare to the best of my knowledge to Bindura University of Science Education that this dissertation is my original work and all materials and academic sources of information other have been duly acknowledged. I also declare that this current work has not been submitted to any other academic institution for the purposes of an academic merit.

Signed 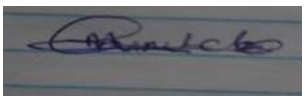 Date 30/06/2025

DEDICATION

I dedicate this academic work to my family who have been there every step of the way. My sincere gratitude goes to my colleagues for their unwavering support.

ACKNOWLEDGEMENTS

I would like to thank my supervisor, Dr N. Muchanyereyi for working with me and giving me expert guidance in performing this research study. My sincere gratitude goes to the Bindura University of Science Education Laboratory staff for their contributions in making the research possible and successful. Finally, I offer my thanks to the Almighty God for all the blessings he has bestowed upon me.

Table of Contents

List of Tables

List of Figures

Abbreviations

AC - activated carbon

FTIR – fourier transform infrared spectroscopy

NP - nanoparticle

pHzpc – zero-point charge pH

SSHAC – sunflower seed husk activated carbon

Abstract

The escalating levels of heavy metal contamination in water bodies represent a significant global environmental concern. Among these pollutants, lead (II) ions are particularly hazardous due to their high toxicity and potential to accumulate in living organisms, leading to severe health issues. This study investigated the absorptive removal of lead from aqueous solutions using a novel sunflower seed husk activated carbon $CoFe_2O_4$ composite. Due to the rising levels of Lead in water bodies due to mining, leaded petrol and battery desposal, the following disorders have resulted as a responses to lead which include cardiovasicular, reproductive and renal disorders hence its removal is needed so this research focuses on that. The composite was synthesized via the coprecipitation method and characterized using Fourier Transform Infrared Spectroscopy (FTIR) and zero-point charge analysis. The adsorption kinetics were evaluated using pseudo-first-order and pseudo-second-order kinetic models, with the pseudo-first-order model providing a better fit (R^2 = 0.9389) compared to the pseudo-second-order model (R^2 = 0.8871). The adsorption isotherms were analyzed using Langmuir and Freundlich models, with the Langmuir model exhibiting a superior fit (R^2 = 0.996) compared to the Freundlich model (R^2 = 0.930). The results demonstrate the potential of sunflower seed husk activated carbon $CoFe_2O_4$ composite as an effective adsorbent for the removal of lead from aqueous solution

CHAPTER 1: INTRODUCTION

1.0 Background

The escalating contamination of global water resources by a myriad of pollutants poses a significant threat to environmental integrity and public health. Rapid industrialization, intensive agricultural practices, and expanding urbanization are primary contributors to the discharge of hazardous substances into aquatic ecosystems (UNICEF & WHO, 2019). Among the most deleterious contaminants are heavy metals, which are characterized by their persistence, non-biodegradability, and tendency to bioaccumulate within the food chain (Tchounwou et al., 2012). Lead (II) ions, in particular, are recognized as highly toxic heavy metals, even at trace concentrations, and their pervasive presence in water bodies is a matter of grave concern worldwide.

Lead (II) can enter water systems through various anthropogenic pathways, including effluents from battery manufacturing, mining operations, smelting industries, pigment production, and the corrosion of lead-containing pipes in aging water distribution networks (Jaishankar et al., 2014; WHO, 2022). Once ingested, lead (II) can cause severe health issues, including neurological damage, particularly in children, leading to developmental delays and learning disabilities. It also adversely affects the renal, cardiovascular, and reproductive systems in adults (Needleman, 2004; Flora et al., 2012). The World Health Organization (WHO) has set a provisional guideline value of 0.01 mg/L for lead in drinking water, highlighting the critical need for effective remediation strategies to reduce its concentration to safe levels (WHO, 2022).

Numerous conventional methods have been employed for the removal of lead (II) from contaminated water, such as chemical precipitation, ion exchange, membrane filtration, reverse osmosis, and electrochemical treatment (Fu & Wang, 2011;Gunatilake, 2015). While these techniques can be effective to varying degrees, they often suffer from significant drawbacks. For instance, chemical precipitation can generate large volumes of hazardous sludge requiring further disposal, ion exchange resins can be expensive and may suffer from interference by other ions, and membrane-based processes often have high operational costs and are prone to fouling Kurniawan et al., 2006; Barakat, 2011). These limitations necessitate the exploration of more cost-effective, efficient, and environmentally benign alternatives for lead (II) remediation.

Adsorption has emerged as a highly promising technique due to its simplicity of design, ease of operation, high efficiency in removing pollutants even at low concentrations, and the potential for adsorbent regeneration and reuse (Bhatnagar et al., 2013). Activated carbon (AC) is one of the most widely used adsorbents owing to its large surface area, well-developed porous structure, and versatile surface chemistry (Dąbrowski, 2001). However, the high cost of commercial activated carbon, often derived from non-renewable sources like coal, has spurred research into the development of low-cost adsorbents from abundant and renewable precursors, particularly agricultural wastes (Mohan et al., 2014). Sunflower seed husks (SSH), an agro-industrial byproduct generated in substantial quantities, represent a lignocellulosic material that can be effectively converted into activated carbon, offering a sustainable and economical alternative (Foo & Hameed, 2011).

To further enhance the adsorption capacity and facilitate the easy separation of adsorbents from treated water, the development of composite materials has gained

considerable attention. Magnetic nanoparticles, such as cobalt ferrite ($CoFe_2O_3$), have been investigated for their potential in water treatment due to their strong magnetic properties, chemical stability, and ease of separation using an external magnetic field (Reddy & Lee, 2013). Incorporating magnetic nanoparticles like $CoFe_2O_3$ into the porous structure of activated carbon can yield a composite adsorbent with synergistic benefits: the high surface area and porosity of activated carbon for efficient lead (II) uptake, and the magnetic properties of $CoFe_2O_3$ for convenient post-treatment separation, thereby avoiding issues like adsorbent loss and the need for filtration or centrifugation (Zhang et al., 2010).

The synthesis of sunflower seed husk activated carbon (SSHAC) and its subsequent modification with $CoFe_2O_3$ nanoparticles to form a magnetic composite (SSHAC/$CoFe_2O_3$) is hypothesized to produce an effective adsorbent for the removal of lead (II) ions from aqueous solutions. The porous nature of SSHAC is expected to provide ample active sites for lead (II) adsorption, while the $CoFe_2O_3$ component will impart magnetic separability and potentially contribute to the overall adsorption capacity through its own surface functionalities (Gao et al., 2009). This approach aligns with the principles of green chemistry and circular economy by valorizing agricultural waste into a high-value material for environmental remediation.

1.1 Problem Statement

Water pollution by heavy metals has become one of the rising concerns because it affects the quality of water which leads to many diseases when consumed by humans and animals. The treatment of heavy metals is of special concern due to their uprising and persistence in the environment due to the industrialization. In most developing countries, people and animals tend to drink untreated water which is polluted with heavy metals. Recent researches have shown much evidence that lead

as one of the heavy metals pose a health risk to humans and the environment even in low concentration on the metal ions due its toxicity. Exposure to lead causes damage to the central nervous system, kidneys and it also affect the haemal synthesis and other biochemical processes. Heavy metal removal from inorganic effluent can be achieved by conventional treatment processes and these include chemical precipitation, coagulation, complexation, activated carbon adsorption, ion exchange, solvent extraction, foam flotation, electro-deposition, cementation, and membrane operations. These methods are effective for the removal of heavy contaminants however, these methods have several drawbacks which include high time consumption, often lead to the concentration of toxins which are difficult to handle and dispose and relatively high costs of operation. This has led to the modification of magnetic nanoparticles which remove the heavy metals effectively even at trace levels and also that they are easy to separate from solution after treatment by applying an external magnet.

1.2 Justification

Sunflower seeds husk is considered as waste in the environment hence, using these husks in the generation of an adsorbent for the removal of lead in aqueous solution will be a waste beneficiation, which in the process reduces their disposal to the environment mainly from the food industry therefore combating another pollution problem. Literature shows several methods of treating waste water but developing an effective low-cost adsorbent will result in reduction in drinking water treatment cost, reduction of heavy metal contamination of water bodies, thus reviving the ecosystem and increase in recreational value of water bodies and to some extent relieving governments of the health care burden. Several methods have been used for the removal of lead such as filtration and reverse osmosis but problem is

production of concentrated toxic sludge which in some processes in difficult to separate and causes a new problem of their concentrated toxicity if they are not disposed well. The possibility of preparing ferrites in the form of nanoparticles has created a gap in water treatment due to their nanometer size, super paramagnetic properties and a high-surface to-volume ratio.

Literature shows that the adsorption of lead on activated carbon can be significantly increased by treatment with various metal oxides. The use of spinel ferrites which have a good degree of magnetism is implemented and can be easily separated from solution by use of a magnet and makes it easy for separation from the treated water by use of simple magnet which is not only cost effective but less toxic than the other methods. The fusion of nano-chemistry and naturally occurring biosorbents gives the material properties which are desirable and these properties include increase capacity for lead removal, increased surface area, and chemical stability of the sorbent as it makes it difficult to be decomposed.

1.3 Aim

To synthesize cobalt ferrite nanoparticles modified with sunflower seeds husk and to systematically evaluate its efficacy for the adsorptive removal of lead (II) ions from aqueous solutions.

1.4 Objectives

1. To prepare activated carbon from sunflower seeds husk.

2. To synthesize cobalt ferrite nanoparticles modified with sunflower seeds husk.

3. To characterize the modified nanoparticle using Fourier Transmission Infrared Spectroscopy.

4. To conduct optimization experiments in determining the effect of pH, contact time, adsorbent dosage and initial concentration on the adsorption of lead (II) ions.

CHAPTER 2: LITERATURE REVIEW

The escalating levels of heavy metal contamination in water bodies represent a significant global environmental concern. Among these pollutants, lead (II) ions are particularly hazardous due to their high toxicity and potential to accumulate in living organisms, leading to severe health issues. Industrial activities such as mining operations and the discharge of inadequately treated wastewater are primary sources of lead (II) ion contamination in aquatic environments (Zhang et al., 2020).

The presence of these ions poses substantial environmental and public health challenges, underscoring the urgent need for effective remediation strategies. However, these techniques often suffer from limitations such as high operational costs, reduced efficiency at lower contaminant concentrations, and the potential generation of secondary pollutants, which can further complicate the treatment process. These drawbacks have spurred considerable research into more sustainable and efficient alternatives, with adsorption emerging as a particularly promising approach. Adsorption offers several advantages, including its high removal efficiency, ease of operation, and the potential for application in situ.

Furthermore, the use of low-cost, readily available materials as adsorbents aligns well with the principles of sustainability and environmental responsibility. Sunflower seed husks, an abundant agricultural waste generated from oilseed processing, have garnered attention as a cost-effective and environmentally friendly precursor for activated carbon production. The vast quantities of this waste material produced annually make it a sustainable resource for the development of adsorbents. Utilizing sunflower seed husks not only provides a low-cost adsorbent but also addresses the environmental burden associated with agricultural waste disposal, promoting a

circular economy approach.

Fig 2.1 Sunflower seed husks, an abundant agricultural waste used as a precursor for activated carbon in heavy-metal adsorption studies.

In parallel, cobalt ferrite ($CoFe_2O_4$) nanoparticles, a magnetic material, have shown significant potential in water treatment applications due to their high surface area, remarkable stability, and the crucial ability to be easily separated from treated water using an external magnetic field. $CoFe_2O_4$ nanoparticles can function both as adsorbents and as catalysts in advanced oxidation processes. The magnetic

property of $CoFe_2O_4$ is particularly advantageous as it allows for straightforward separation and recovery of the adsorbent after the treatment process, thereby preventing secondary pollution and enabling material reuse. The combination of sunflower seed husk activated carbon with $CoFe_2O_4$ nanoparticles into a composite material is hypothesized to offer synergistic benefits for the removal of lead (II) ions from aqueous solutions. It is anticipated that the activated carbon component will provide a high surface area with numerous active sites for lead (II) ion adsorption, while the incorporation of $CoFe_2O_4$ nanoparticles will impart magnetic separability to the composite and potentially enhance the adsorption process through favourable surface interactions. This approach aims to capitalize on the strengths of both materials, potentially leading to a more efficient and practically viable solution for the remediation of lead (II) ion contaminated water. This literature review seeks to provide a comprehensive overview of the current research focused on the application of sunflower seed husk activated carbon / $CoFe_2O_4$ composite for the removal of lead (II) ions from aqueous solution. The review will cover aspects such as the preparation and characterization of the individual components and the composite, the evaluation of its adsorption performance, the influence of various experimental factors, and potential future directions in this field.

2.1 Synthesis of sunflower seed husk activated carbon/ $CoFe_2O_4$

Sunflower seed husks waste from oil processing and snack production are collected for the production of activated carbon. Prior to their conversion into activated carbon, sunflower seed husks typically undergo several pre-treatment steps to remove impurities and prepare them for the subsequent carbonization and activation processes. Common pre-treatment methods include washing the husks with water to eliminate surface contaminants such as soil and dust. This washing step ensures

that the subsequent processes are not hindered by the presence of particulate matter. Following washing, the husks are usually dried to reduce their moisture content, which is crucial for efficient thermal conversion. In some cases, the dried husks may be crushed and sieved to obtain a more uniform particle size, which can improve the consistency and efficiency of the activation process.

Proper pre-treatment is essential for removing unwanted materials and ensuring effective carbonization and activation, ultimately leading to a high-quality activated carbon product. Activated carbon can be prepared from sunflower seed husks using either physical or chemical activation methods. Physical activation typically involves two main steps: carbonization followed by activation. In the carbonization step, the pre-treated sunflower seed husks are heated in an inert atmosphere, such as nitrogen or argon, at high temperatures (typically between 600 and 900 °C) to remove volatile compounds and produce a carbon-rich char. The subsequent activation step involves exposing the carbonized material to an activating agent, usually a gas like steam or carbon dioxide, at even higher temperatures (ranging from 800 to 1100 °C). This process develops the porous structure of the activated carbon by creating new pores and enlarging existing ones. After being dried, the activated carbon is added to the solution of the Co^{2+} and Fe^{3+} salts (e.g. nitrates) are co-precipitated or impregnated onto the biochar surface, then heated to form $CoFe_2O_4$ nanoparticles fixed on the carbon matrix. This yields a composite with high surface area and magnetic separability. (Shabelskaya et al., 2023) noted that embedding ferrite particles in biochar combines the “developed surface due to organic carrier and magnetic or semiconductor properties due to inorganic component”. The magnetized AC can be easily collected by a magnet after adsorption.

2.2 Characterization of SSHAC/ $CoFe_2O_4$

The composite material is characterized using a range of techniques to confirm the presence and interaction of both the activated carbon and the nanoparticles. X-ray Diffraction (XRD) analysis can confirm the presence of both the amorphous carbon phase, characteristic of activated carbon, and the crystalline spinel phase of $CoFe_2O_4$ (Sonja et al., 2019). Fourier Transform Infrared Spectroscopy (FTIR) is used to identify the characteristic functional groups of the activated carbon and the vibrational modes associated with $CoFe_2O_4$. Any shifts or changes in these peaks can indicate interactions between the two components in the composite.

2.3 Absorptive Studies of Pb(II) onto the Composite

2.3.1 Effect of pH

The pH controls Pb speciation and surface charge of the adsorbent. At low pH, competition from H^+ ions and protonation of adsorbent functional groups inhibits Pb uptake. Removal typically increases as pH rises (often peaking around 5–7) because deprotonated sites bind Pb^{2+} more strongly. For example, coconut shell AC reached higher Pb^{2+} adsorption at pH 5–6, while very high pH (>10) led to $Pb(OH)_2$ precipitation and lower apparent uptake. (Chowdhury et al., 2022) note that many natural adsorbents show optimal removal in the mildly acidic neutral range (pH ~5–7). Above this, Pb begins to form hydroxide precipitates, confounding adsorption measurements.

2.3.2 Effect of contact time

Adsorption typically exhibits fast initial uptake followed by a slower approach to equilibrium. Kinetic studies usually show that equilibrium is attained within tens of minutes to a few hours. For example, one study with orange bark reported

equilibrium 70% Pb removal was reached 7within ~10,800 s (3 hours) at moderate conditions. A pseudo-second-order kinetic model (implying chemisorption) often fits the data best. (Abdulhusain et al., 2023). found that Pb(II) adsorption on raw husk followed 18 20 20 pseudo-second-order kinetics with high R^2 (≈0.99), indicating rate-limiting chemical bonding processes. In practice, reaction times of 30–60 min are common to achieve >90% of equilibrium removal.

2.3.3 Effect of adsorbent dosage

Increasing the adsorbent mass generally increases the percentage removal, as more binding sites become available. However, the adsorption capacity per unit mass (q_e) may decrease at high dosage due to aggregation or unsaturation. In the sunflower-husk study, raising the sorbent dose from 0.5 to 8 kg/m³ (0.05 to 2 g per 100 mL) dramatically increased Pb removal from ~16% to ~70%. A similar trend is seen in many biosorption experiments: beyond an optimal dose, further addition yields diminishing returns in % removal. Thus, it is common to optimize dosage to balance efficiency and economy.

2.3.4 Effect of initial Pb(II) concentration

The starting metal concentration influences the driving force for adsorption. At low [Pb], removal percentage can be high (since few ions saturate the sites). As initial [Pb] increases, more Pb is adsorbed in absolute terms (higher q_e) but the removal % may drop if active sites become limiting. Most studies report an increase in q_e with higher [Pb] until plateau. For example, Azouaoua et al. observed that raising initial Pb^{2+} from 10 to 600 mg/L (in orange bark tests) increased q_e accordingly, and the Langmuir model could then estimate maximum q_{max}. When designing removal processes, one must consider the influent [Pb] higher concentrations typically

require more adsorbent or longer contact to achieve comparable % removal.

2.4 Adsorption Isotherms

Adsorption isotherms are mathematical models that describe the equilibrium relationship between the amount of adsorbate adsorbed onto the surface of the adsorbent and the concentration of the adsorbate in the liquid phase at a constant temperature. These models provide crucial insights into the adsorption mechanism and the surface properties of the adsorbent. Several isotherm models are commonly used to fit experimental adsorption data. The Langmuir isotherm model assumes monolayer adsorption onto a homogeneous surface with a finite number of identical adsorption sites. Fitting the Langmuir model to experimental data can yield parameters such as the maximum adsorption capacity of the composite, which represents the theoretical maximum amount of lead (II) ions that can be adsorbed per unit mass of the adsorbent under specific conditions. The Freundlich isotherm model describes multilayer adsorption on a heterogeneous surface with a non-uniform distribution of adsorption sites. The Freundlich model provides information about the adsorption intensity and the degree of surface heterogeneity. A study on activated carbon from sunflower seed shells for the removal of Pb(II) found that the adsorption models by (Foo & Hameed, 2009) aligned with both the Freundlich (R^2 = 0.9976) and Langmuir (R^2 = 0.966) isotherm models, indicating a high sorption capacity. Another study using modified sunflower seed husks activated carbon for the removal of several heavy metals, including lead (II), found that the adsorption process conformed to the Langmuir adsorption isotherm.

2.5 Adsorption kinetics

Adsorption kinetic models are used to understand the rate of adsorbate uptake and

the mechanism of the adsorption process over time. These models help in determining the rate-limiting steps involved in the adsorption of adsorbate. The pseudo-first-order (PFO) model assumes that the rate of adsorption is proportional to the number of unoccupied adsorption sites on the adsorbent surface. Fitting the PFO model to experimental data can provide an initial estimate of the adsorption rate constant. The pseudo-second-order (PSO) model, in contrast, assumes that the rate-limiting step is chemical adsorption involving valence forces through sharing or exchange of electrons between the adsorbate and the adsorbent. The PSO model often provides a better fit for the adsorption of heavy metal ions onto various adsorbents, suggesting that chemisorption might be the dominant mechanism. Another important kinetic model is the intra-particle diffusion model, which examines the possibility that the diffusion of the adsorbate molecules within the pores of the adsorbent material is the rate-controlling step. Studies using sunflower seed husk biochar for copper removal found that the adsorption kinetics of Cu(II) fitted well to the pseudo-second-order equation, indicating a strong biosorbent. Similarly, a study on activated carbon from sunflower seed shells for the removal of Pb(II), Cd(II), and Cr(III) also found that the adsorption behaviour aligned with both Freundlich and Langmuir isotherms. While specific kinetic models for the composite of sunflower seed husk activated carbon and CoFe2O4 for lead (II) removal are not explicitly mentioned in the provided snippets, the prevalence of PSO model fitting in related studies suggests it would be a relevant model to consider for this composite as well (Awad, 2014).

CHAPTER 3: MATERIALS AND METHODS

3.1 Introduction

This chapter points out on steps taken to meet the objective of the study. This includes synthesis of the cobalt ferrite-NP modified with sunflower seeds husks, characterization and batch absorption studies.

3.2 Materials

3.2.1 Reagents and Chemicals

All chemicals used are analytical grade (AR grade) supplied by Astra Chemicals PVT Ltd and deionized water was obtained at BUSE sanitizer and detergents plant. Sulphuric acid 98%, hydrochloric acid 33%, nitric acid 70%, phosphoric acid 85%, sodium hydroxide, sodium bicarbonate, iron chloride, cobalt chloride, sodium chloride, lead nitrate, sunflower seed husks and ethanol 95%.

3.2.2 Instruments

Fourier Transmission Infra – Red spectrometer (FTIR), Atomic Absorption Spectrometer (AAS) and pH

3.3 Synthesis of cobalt ferrite-NP modified with sunflower seed husks

3.3.1 Preparation of activated carbon from sunflower seeds husk (chemical activation method)

Chemical activation was carried out by 50% phosphoric acid (H_3PO_4) as it increases the porosity of the carbon structure during the acid treatment. Sunflower seeds were bought at Mbare Musika, and then crushed into powder. The crushed powder was boiled in deionized water and cooled. The procedure was repeated until the

supernatant was colourless. The washed crushed powder was rinsed with 1% HCl, then washed again with deionized water until the wash water became colorless. The powder was dried at 80 °C for 24 hours in a hot air oven to get rid of moisture and volatiles. Concentrated sulphuric acid was added to the pretreated sunflower seed waste powder in the ratio of 1:2 (w/v). It was washed again with deionized water continuously to remove free acid and soaked in 1% sodium bicarbonate solution overnight to neutralize the acid, and then washed with deionized water and dried at 80 °C in hot air oven for 24 hours. The dried material was placed in a muffle furnace for thermal activation at 500 °C for 1 hour. The powder was cooled and washed with deionized water and dried at same conditions as mentioned above. The activated carbon was sieved using the standard mesh of size 250 µm and stored in a vacuum desiccator for further use.

3.3.2 Synthesis of cobalt ferrite nanoparticles modified with activated carbon

About 12. 093 g of Ferric chloride and 7.276 g Cobalt chloride were mixed in deionized water. 250 ml deionized water was used as a solvent in order to avoid the production of impurities in the final product. Sodium hydroxide (3 M) solution was prepared and 25 ml was added slowly to the salt solution dropwise. The pH of the solution was constantly monitored as NaOH solution was being added. Reactants were constantly stirred using a magnetic stirrer until a pH level of 11-12 was reached. About 30 g of the prepared activated carbon was added to the solution as a surfactant and coating material. The liquid precipitate was heated to 80 °C and stirred for one hour and the product was then cooled to room temperature. The precipitate was washed twice to get free particles from sodium and chlorine compounds and then with ethanol to remove the excess surfactant from the solution. To isolate the supernatant liquid centrifuge, the conical flask contents for fifteen

minutes at 5000 rpm. The supernatant liquid was decanted and centrifuged until a thick black precipitate is observed. The precipitate was dried overnight at 100 °C. The product was grounded into a fine powder. At this stage the product ($CoFe_2O_4$) contained some associated water, heat at 600 °C for ten hours to remove excess water. A strong magnet was used to confirm if the synthesized product is magnetic.

3.4 Characterization of $CoFe_2O_4$/ AC

3.4.1 Determination of pHzpc and pH

The pH meter (Milwaukee MW150 pH) was calibrated using pH 4, pH 7 and pH 9 buffers obtained from astra chemicals Pvt Ltd. The pH value at zero charges (pHpzc) was obtained by the Mular - Robert titration method (Hoang et al., 2010). 1 g of $CoFe_2O_4$/AC was put into 100 mL of 0.1 M KCl solution with pH adjustment in the range from 2 to 12 done by the addition of 0.1 M NaOH or 0.1 M HCl (pH_{iS}). The flasks then were sealed and shaken in 24 hours before recording the final solution pH (pH_{fs}). The ΔpH values ($\Delta pH = pH_{is} - pH_{fs}$) were orchestrated against pH_{iS}. The pHpzc represents the intersection point of the curve and ΔpH.

3.4.2 Characterization using FTIR

The $CoFe_2O_4$/ AC was characterized before and after reaction using FTIR (FTIR ThermoScientific Nicolet 6400) to determine the functional groups present (Kumar et al. (2019)). The crystals were mixed with KBr which is used as the background material in the ratio 1: 100 respectively through grinding using a mortar and pestle. A significant amount of the sample enough to cover the bolt was added, pressed to a transparent disk and then placed into a FTIR sample holder and analysed using the FTIR spectrometer in a range between 500 to 3600 cm^{-1}.

3.5 Batch Absorption Studies

In batch absorption studies, lead adsorption was investigated under following parameters: the effect of pH, adsorbent dosage, initial metal ion concentration and contact time. The experiment was done with a constant volume of Pb^{2+} (30 mL). Two control sample were included in every experiment set up which were one with $CoFe_2O_4$ / AC and the other one with raw sunflower seeds husks was used as the control. The adsorption capacity (q) is obtained by calculation using the following formula.

$$q = \frac{(C0 - Ct)V}{m} \quad \text{……………………………………………………} \quad 3.1$$

Where: C_0 = initial Pb^{2+} concentration (ppm)

C_t = Pb^{2+} concentration at time(t) (ppm)

V = volume of solution

m = mass of $CoFe_2O_4$/AC (mg)

3.5.1 Isotherm Modelling

The distribution of Pb^{2+} between the liquid state and the solid state can be provided by the isotherm parameters (Hoang et al., 2020). Langmuir and Freundlich models were utilized as analysers for the gathered experimental data. The equations of Langmuir and Freundlich models are described as shown in (3.2) and (3.3).

$$q_e = q_m K_L C_e / 1 + K_L C_e \quad \text{………………………………………………} \quad 3.2$$

$q_e = K_f C_e^{(1/n)}$ …… 3.3

where C_e and q_e are the Pb^{2+} concentration and the adsorption capacity (mg/g) at equilibrium (ppm), respectively, q_m is the Langmuir adsorption capacity (mg/g), K_L is the Langmuir constant (L/mg), K_f is the Freundlich coefficient (mg/g) and n is the adsorption intensity.

The nature of the Langmuir isotherm was studied using the equation (3.4) shown below.

$$q_t = \frac{1}{1 + KCo} \quad \text{…… 3.4}$$

where q_t is the separation factor, K is the Langmuir constant and C_o is the initial Pb(II) concentration in mg/L (Muhammad., et al 2019).

3.5.2 Adsorption kinetics

The adsorption kinetics of Pb^{2+} onto $CoFe_2O_4$/AC were clarified through the contribution of the pseudo-first-order (3.5) and pseudo-second-order models (3.6).

$\ln (q_e - q_t) = \ln q_e - k_t t$ …… 3.5

$t / q_t = 1 / k_2 q_e^2 + t / q_e$ …… 3.6

where q_t (mg/g) and q_e (mg/g) are the adsorption capacity at time (t) and at equilibrium, respectively, k_1 (min^{-1}) is the first order rate constant, and k_2 (g/mg·min) is the second-order rate constant.

3.5.3 Preparation of stock solutions and the calibration standards

Prepare 1000 ppm of stock solution of lead dissolving $Pb(NO_3)_2$ in 1000 ml of deionized water. The mass of the salt for the preparation of the stock solution is calculated using the formula:

$$\text{Mass of the salt(g)} \frac{\text{Mr(metal salt)}}{\text{Ar(metal atom)}} \quad \text{……………………………………} \; 3.7$$

The working solutions are also going to be prepared from the stock solution

3.5.4 Effect of pH in the adsorption of Pb(II)

The efficiency of the $CoFe_2O_4$/AC in Pb^{2+} ions adsorption was investigated in the 4 - 9 pH range at constant volume of 50 mL of 5 ppm Pb^{2+} ion solution and 100 mg adsorbent. The pH was adjusted to the desired values by addition of dilute 0.1 M hydrochloric acid (HCl) and 0.1 M sodium hydroxide (NaOH) using a dropper. The samples were occasionally stirred at 1500 rpm for the minutes. After 30 minutes, the adsorbent was removed by filtration from the beaker and the remaining solution was used for determining the change in Pb^{2+} ions concentration by collecting 5 mL sample of the solution and measuring it using previously calibrated AAS.

3.5.5 Effect of contact time

The Pb^{2+} ion adsorption efficiency by the adsorbent was examined by varying the

contact time over the range of 0 - 180 minutes. A volume of 50 mL, adsorbent dosage of 100 mg and Pb(II) concentration of 5 ppm were used. The samples were then stirred and at every 30 minutes' intervals 5 mL aliquots of sample was collected and transferred to the AAS and analysed for the change in Pb^{2+} ion concentration.

3.5.6 Effect of initial Pb^{2+} concentration

The effect of initial Pb^{2+} ion concentration on adsorption by adsorbent was determined by adding 50 mL solutions of varying initial Pb^{2+} ion concentrations from 5 -25 ppm range and constant adsorbent dosage of 100 mg. The samples were stirred for 60 minutes and after that they were filtered to remain with the solution. The remaining solution was used for analyses to determine change in Pb^{2+} ion concentration. A 5 mL was collected from the filtered solution and was transferred for the test of the level of adsorption using the previously calibrated AAS.

3.5.7 Effect of adsorbent dosage on Pb^{2+} adsorption.

The effect of adsorbent dosage was investigated by ranging dose of adsorbent from 20 mg -100 mg of adsorbent was added to a constant volume of 50 mL of Pb^{2+} ion solution and Pb^{2+} concentration of 5 ppm in a set of 50 ml beakers. The samples were then magnetically stirred for 30 minutes. After 30 minutes, they were filtered and the remaining solutions were collected to determine the change in Pb^{2+} ion concentration by collecting 5 mL of each of the solutions and transferred to the AAS.

CHAPTER 4: RESULTS AND DISCUSSION

4.0 Introduction

The section is focused on presentation of experimental findings and their discussion in comparison to the information from literature. The results are presented in various forms including graphs and tables.

4.1 Characterization Result

4.1.1 FTIR Analysis

Figure 4.1 shows the FTIR spectra of SSHAC/$CoFe_2O_4$.

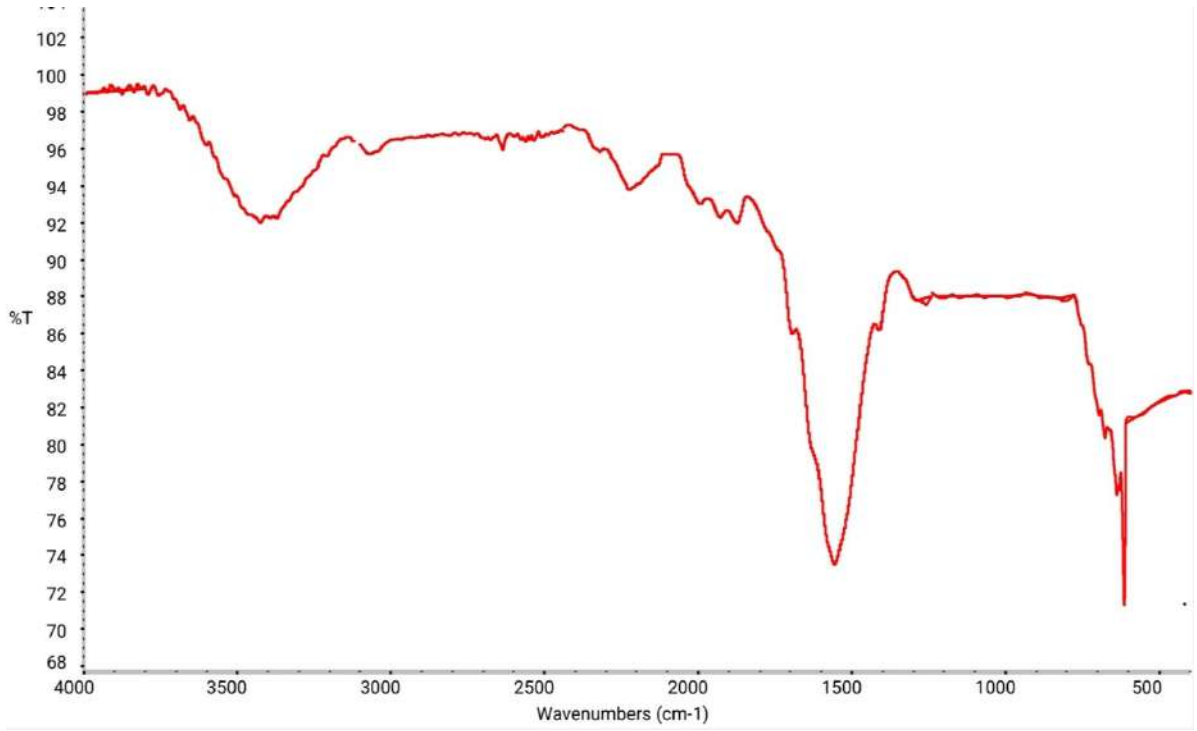

Fig 4.1 FTIR of SSHAC/$CoFe_2O_4$.

The FTIR spectrum exhibits characteristic peaks. A broad and intense band around 3400 cm^{-1} corresponds to O-H stretching vibrations, this suggests the presence of

hydroxyl groups which plays a major role in metal complexation. The peak observed near 1600 cm^{-1} is attributed to C=O stretching vibrations from carbonyl or carboxyl groups. A peak around 1380 cm^{-1} indicates the presence of C-O bending vibrations while a band around 1100 cm^{-1} can be assigned to C-O-C or phenolic -OH groups. Distinct peaks 580-700 cm^{-1} are associated to Fe-O and Co-O stretching vibrations confirming the presence of spinel ferrite ($CoFe_2O_4$) phase.

4.1.2 Point Zero Charge Analysis

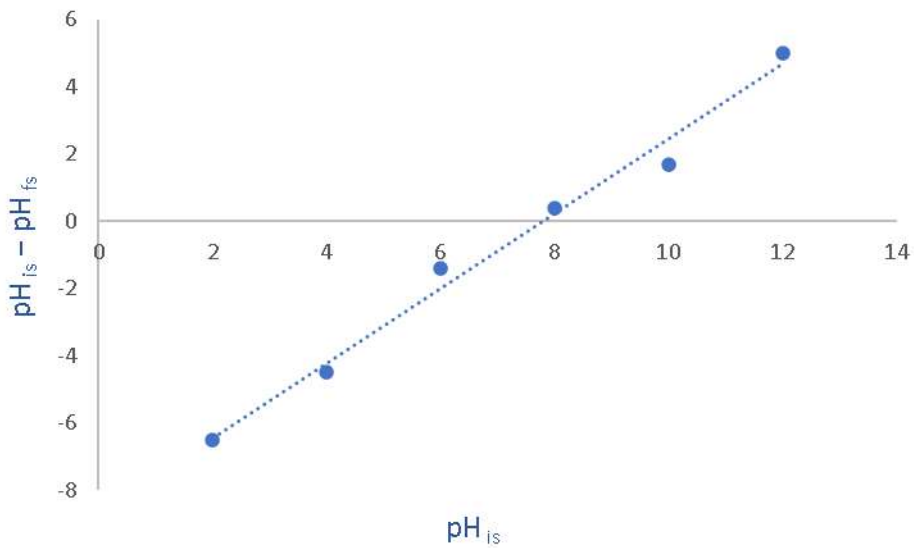

Fig 4.2 Zero Point Charge for SSHAC/$CoFe_2O_4$.

From the graph above, the value of pH_{PHZ} is identified as the point where $pH_{is} - pH_f = 0$, which occurs between pH 6 and 8(Figure 4.2). According to the graph pH_{PHZ} is 7.62 which is different from that obtained by (Hoang et al., 2020) because of the 50% H_3PO_4 used for making activated carbon. At this pH, the surface charge of composite is neutral and below this pH the surface is positively charged which enhances the adsorption of anionic species. However, above this pH, the surface becomes negatively charged, which favours the adsorption of cationic species such as Pb^{2+}. This is a characteristic vital in designing effective heavy metal adsorption in aqueous solutions for example, since Pb(II) is divalent cation, its optimum adsorption would occur above pH_{PHZ} where the surface is negatively charged favouring electrostatic attractions (Aljeboree et al., 2017; Foo & Hameed, 2010). The fundings are consistent with similar studies on magnetic carbonaceous composites, where metal ferrite components influence the surface charge behaviour thereby enhancing absorptive capacities of the material (Liu et al., 2012).

4.2 Adsorption Studies

4.2.1 Effect of pH in the adsorption of Pb(II)

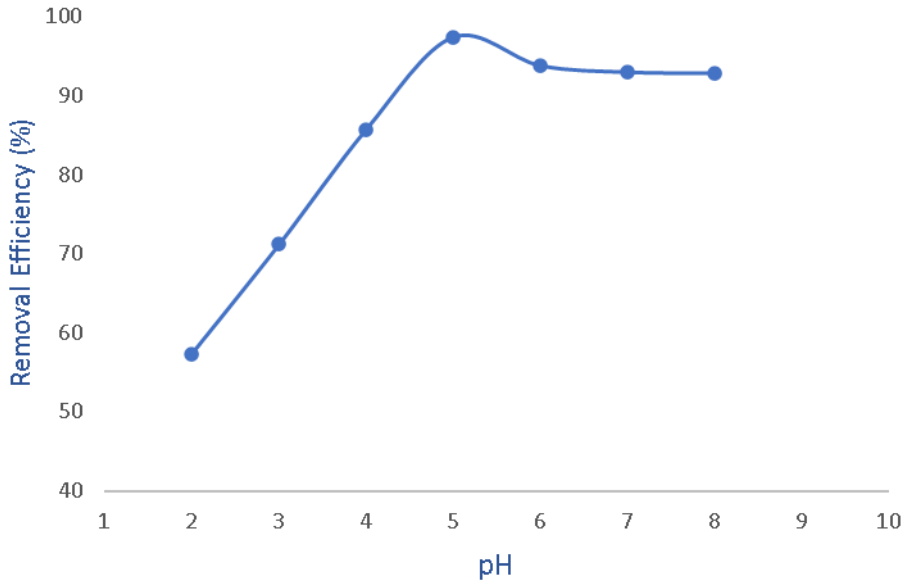

Fig 4.3 Effect of pH in the adsorption of Pb(II)

The removal of efficiency of Pb(II) increased significantly rising from pH 2 to 5 (Figure 4.3), peaking at 97.44% at pH 5. Beyond this pH, the efficiency remained high (>92%) but showed a slight decrease and plateau from pH 6 to 8.

This trend can be explained by the surface charge behaviour of SSHAC/$CoFe_2O_4$ composite. At low pH (e.g., pH 2-3), a high concentration of H^+ ions compete with

Pb^{2+} ions for adsorption sites, reducing Pb(II) uptake (Liu et al., 2012). As the pH increases, the competition from H^{+} diminishes and the surface becomes less positively charged enhancing adsorption though electrostatic attraction (Yahya et al., 2020). The optimum performance is at pH 5 which is close to ideal Pb^{2+} binding on the composite. Above this pH, although the removal remains high the system likely experiences partial precipitation of Pb^{2+} as $Pb(OH)_2$ which contributes to apparent removal (Fu & Wang, 2011).

4.2.2 Effect of contact time

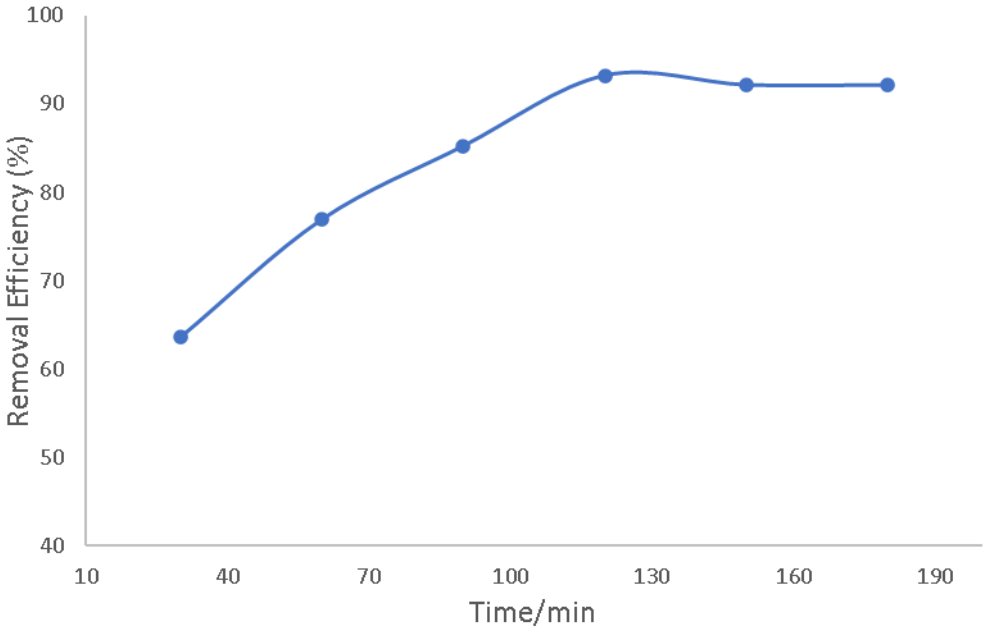

Fig 4.4 Effects of contact time

The effect of contact time was investigated using a constant adsorbent dosage of 100mg/50ml Pb(II) sample (Figure 4.4). The obtained results show a rapid increase removal efficiency within the first 120 minutes reaching a maximum of 93.23%. Beyond 120 minutes, the efficiency plateau slightly indicating that equilibrium has been reached and this behaviour is a characteristic of a typical adsorption process that involves two distinct phases:

1. **Initial rapid phase (0-90 min):** At this stage a large number of active adsorption site are available on the composite surface. Pb(II) ions are quickly adsorbed due to high concentration gradient and electrostatic attraction between Pb^{2+} and the negatively charged surface of the adsorbent at optimal pH (Yahya et al., 2020).
2. **Slower equilibrium phase (90-180 min):** As time progressed, the available active sites became occupied and diffusion into internal pores became the rate limiting step. By 120 minutes the system reached dynamic equilibrium, beyond which no significant increase in removal is observed suggesting that the maximum removal of Pb(II), balancing both efficiency and operational time.

4.2.3 Effect of adsorbent dosage

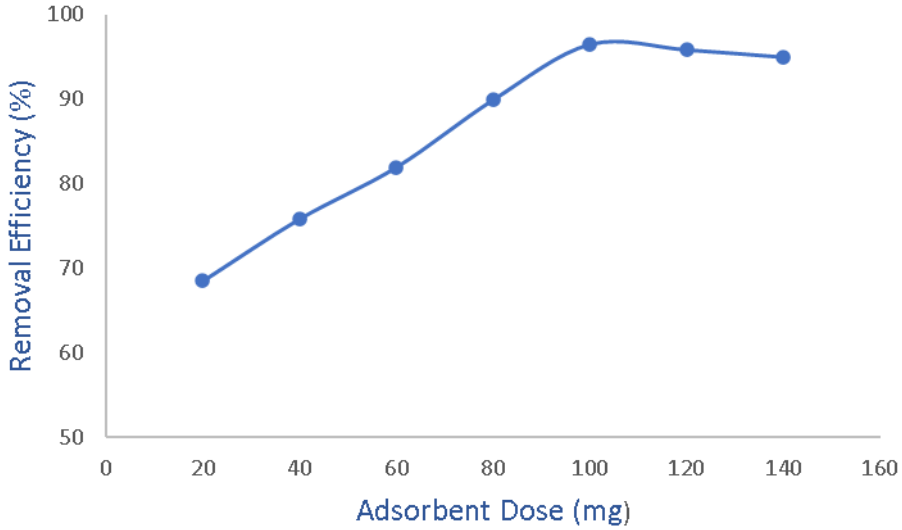

Fig 4.5 Effect of adsorbent dosage

Figure 4.5 shows a clear trend of increasing Pb(II) removal efficiency with increasing adsorbent dose up to 100 mg, where the maximum efficiency of 96.48% is achieved. This is mostly attributed to the greater availability of active surface site for binding Pb^{2+} at high doses (Hoang et al., 2020). The composite`s high surface and magnetic $CoFe_2O_4$ nanoparticles facilitate enhanced metal ion adsorption.

There is a slight decrease in removal efficiency that is observable beyond 100 mg with values dropping from 95.85% and 94.97% at 120 mg and 140 mg respectively.

Particle aggregation reduces the active surface area by blocking the active site (Liu et al., 2012). Moreover, excessive adsorbent can lead to adsorbent-adsorbent interactions causing interference with Pb(II) accessibility resulting in low adsorption efficiency (Sari et al., 2007). The optimum dosage is 100 mg where there is the maximum efficiency.

4.2.4 Effect of initial Pb concentration

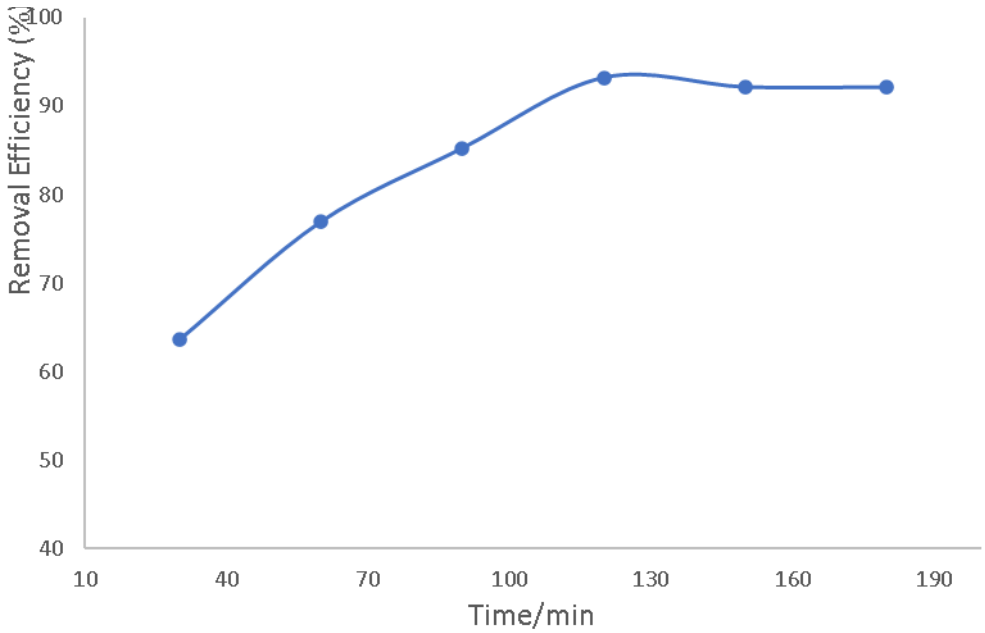

Fig 4.6 Effect of initial Pb concentration

The effect of initial Pb(II) concentration was investigated using a constant adsorbent dosage of 100mg/50ml Pb(II) sample. The results obtained show a decrease trend in the removal efficiency as the initial Pb(II) concentration increases (Figure 4.6). The highest removal efficiency (92.15%) was achieved at a low concentration of 5 ppm while the efficiency declined to 63.56% at 25 ppm.

This inverse relationship is attributed to fixed number of active adsorption sites on the composite surface. At lower concentrations, these sites are sufficient to capture most Pb(II) ions resulting in higher efficiency. However, as the concentration increases more Pb(II) ions are present than the active sites leading to a lower efficiency dure to surface saturation (Fu & Wang, 2011). Additionally, at high concentrations the adsorption process becomes limited by diffusion of Pb(II) ions into internal pores and competitive occupation of active sites mesoporous and microporous structures found in activated carbon-based materials (Liu et al., 2012).

4.3 Adsorption isotherm modelling

For qualitative comparison of the behaviour of adsorbents under several experimental conditions, the adsorption isotherms are important for describing how the adsorbent interacts with the adsorbate including prediction of adsorption parameters.

Two mostly used models are the Langmuir and Freundlich models, so they were selected for the simulation of the adsorption isotherms in this research and for explaining the interactions between Pb(II) ions and SSHAC/$CoFe_2O_4$.

Comparing both fits, the Langmuir model gives a substantially higher correction coefficient (R^2 = 0.996) in (Fig 4.6) than that of Freundlich (R^2 = 0.930) in (Figure 4.7).

This indicates that Pb(II) adsorption of this composite is best described by Langmuir and q_{max} = 17.96 mg/g. Practically the adsorption is efficiently monolayer and nearly homogeneous under these conditions.

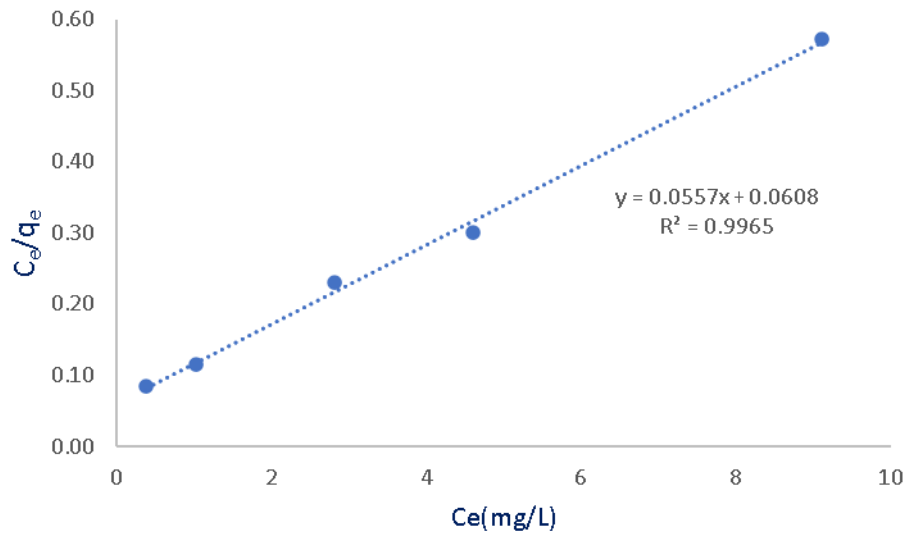

Fig 4.6 The Langmuir adsorption isotherm modelling

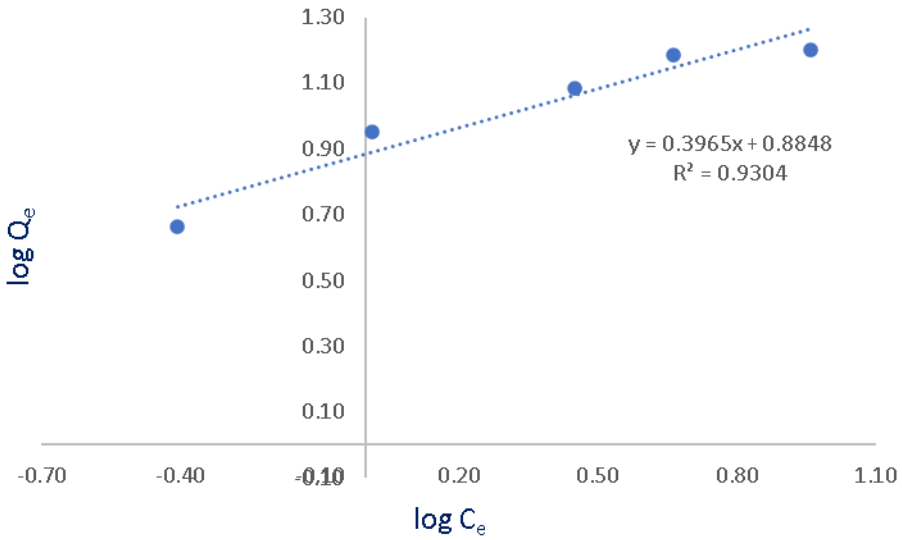

Fig 4.7 The Freundlich adsorption isotherm modelling

4.4 Adsorption Kinetics

Adsorption kinetics describe how fast a solute is taken up by a solid over time. Two common models for solid-liquid adsorption are the pseudo-first order and pseudo-second order rate laws. The pseudo-first order model assumes that the rate of adsorption is proportional to the number of unoccupied sites. The pseudo-second order assumes that chemisorption dominates.

Table 4.1 shows that the R^2 values that were experimentally obtained for pseudo first order kinetics is higher than that of the pseudo second order kinetic model. Due to high value of the correlation coefficient value, R^2 for the pseudo first order plot (Fig 4.8) the adsorption is best fitted the pseudo first order model. The correlation coefficient value, R^2 = 0.8871 (Fig 4.9). this interprets that the rate determining step of the adsorption of Pb(II) on the adsorbent maybe physisorption, the absorbate formed physical bonds with the surface of the adsorbent.

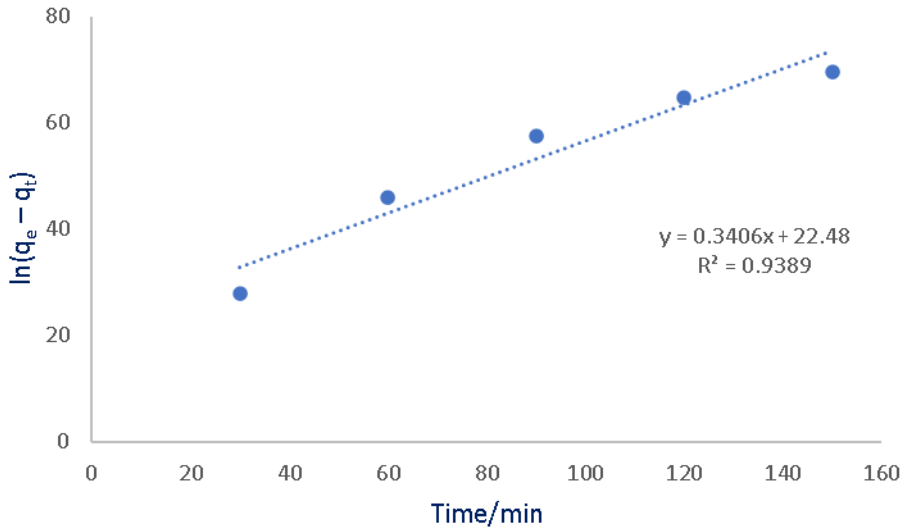

Fig 4.8 Pseudo first order model for the adsorption of Pb(II)

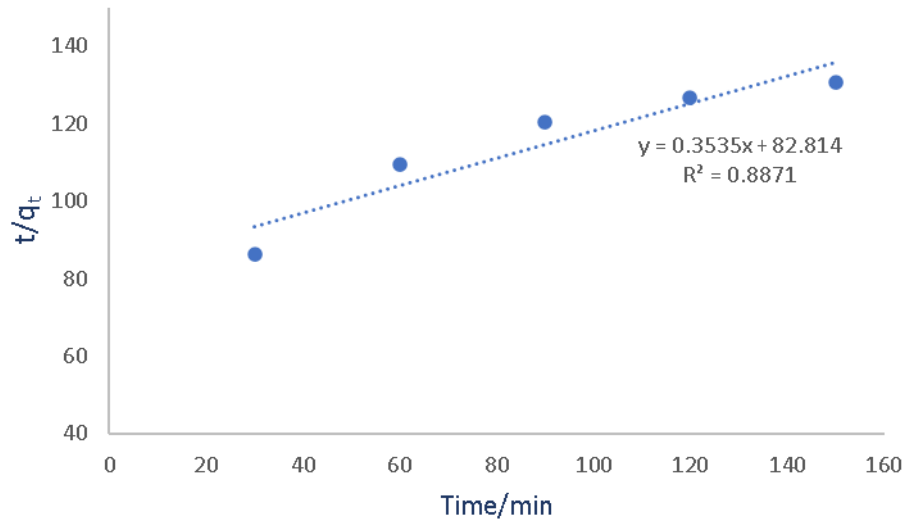

Fig 4.9 Pseudo second order kinetic model for the adsorption of Pb(II)

Table 4.1 Kinetic parameters for 1^{st} and 2^{nd} order

1^{st} order kinetics			2^{nd} order kinetics		
R^2	q_e(mg/g)	k_1(min^{-1})	R^2	q_e(mg/g)	k_2(mg.min)
0.9389	78.1	0.0148	0.8871	150.0	3×10^{-4}

CHAPTER 5: CONCLUSION AND RECOMMENDATIONS

5.1 Conclusion

The experimental data has proven that SSHAC/$CoFe_2O_4$ is effective in the removal of Pb(II) ions in aqueous solution. The research was successful since all the objectives were achieved. The key findings were:

1. The adsorption follows the Langmuir model.
2. The adsorption behaviour follows the pseudo-first order model.
3. The composite works best at pH 5.
4. The FRIR findings confirmed the composite formation with –OH, C=O, C-O, C-O-C or phenolic –OH, Co-O and Fe-O functional groups were present.
5. The zero-point charge showed the surface charge of 7.62.

5.2 Recommendations

Future researches should focus more on studying the regeneration capacity of the adsorbent. More research should be done on the characterization techniques since this research only used FTIR and zero-point charge pH because of the financial constraints. So, the following techniques should be done: XRD, SEM, TEM, TGA among others for best understanding of the properties and structure of the composite. The composite shows an improvement in adsorption and might have negative effects so studies on its effects must be done.

References

Abdulhusain, N. A., & Mokif, L. A. (2023). The removal performance of bio-sorption on sunflower seed husk for copper and lead ions from aqueous solutions. Journal of Ecological Engineering, 24(5), 110 117.

Awad A. (2014). Removal efficiency, metal uptake, and breakthrough curve of aqueous lead ions removal using olive stone waste. Results in Engineering, 22, 2590 -1230, https:doi.org/10.1016/j.rineng. 2024.102311.

Azouaoua, N., Belmedani, M., Mokaddem, H., & Sadaoui, Z. (2013). Adsorption of lead from aqueous solution onto untreated orange barks. Chemical Engineering Transactions, 32, 53–58.

Barakat, M.A. (2011). New trends in removing heavy metals from industrial wastewater. Arabian Journal of Chemistry, 4(4), 361-377.

Bhatnagar, A., Hogland, W., Marques, M., & Sillanpää, M. (2013). An overview of the modification methods of activated carbon for its application in the removal of dilute concentrations of pollutants from water. Chemical Engineering Journal, 219, 499-511.

Chowdhury, I. R., Chowdhury, S., Mazumder, M. A. J., & Al-Ahmed, A. (2022). Removal of lead ions (Pb^{2+}) from water and wastewater: A review on low-cost adsorbents. Applied Water Science, 12(185).

Dąbrowski, A. (2001). Adsorption—from theory to practice. Advances in Colloid and Interface Science, 93(1-3), 135-224.

Flora, G., Gupta, D., & Tiwari, A. (2012). Toxicity of lead: A review with recent updates.

Interdisciplinary Toxicology, 5(2), 47-58.

Foo, K. Y., & Hameed, B. H. (2010). Insights into the modeling of adsorption isotherm systems. Chemical Engineering Journal, 156(1), 2–10.

Foo, K.Y., & Hameed, B.H. (2011). Preparation of activated carbon from sunflower seed husk by P_2O_5 chemical activation for the adsorption of Remazol Brilliant Blue R. Journal of Hazardous Materials, 190(1-3), 930-935.

Fu, F., & Wang, Q. (2011). Removal of heavy metal ions from wastewaters: a review. Journal of Environmental Management, 92(3), 407-418.

Gao, H., Zhao, S., Li, X., & Li, G. (2009). Preparation and characterization of Fe_3O_4/chitosan nanocomposite and its application for removal of Cu(II) from aqueous solution. Journal of Hazardous Materials, 166(2-3), 1175-1180. (Note: Example for magnetic composites, specific $CoFe_2O_3$ refs needed for actual dissertation)

Gunatilake, S.K. (2015). Methods of removing heavy metals from industrial wastewater. Journal of Multidisciplinary Engineering Science Studies, 1(1), 12-18.

Ho, Y. S., & McKay, G. (1999). Pseudo-second order model for sorption processes. Process Biochemistry, 34(5), 451–465. https://doi.org/10.1016/S0032-9592(98)00112-5

Jaishankar, M., Tseten, T., Anbalagan, N., Mathew, B.B., & Beeregowda, K.N. (2014). Toxicity, mechanism and health effects of some heavy metals. Interdisciplinary Toxicology, 7(2), 60-72.

Kurniawan, T.A., Chan, G.Y.S., Lo, W.H., & Babel, S. (2006). Physico–chemical treatment techniques for wastewater laden with heavy metals. Chemical Engineering

Journal, 118(1-2), 83-98.

Li, H., Dong, X., da Silva, E. B., de Oliveira, L. M., Chen, Y., & Ma, L. Q. (2017). Mechanisms of metal sorption by biochars: biochar characteristics and modifications. Chemosphere, 178, 466 478.

Liu, Y., Yang, F., Zhang, H., Yan, L., & Luo, X. (2012). Adsorption of Pb(II), Cd(II) and Cr(VI) from aqueous solution by graphene oxide modified with 1,6-hexanediamine. Chemical Engineering Journal, 229, 444–452.

M. Alkherraz, A. K. Ali, and K. M. Elsherif. Removal of Pb(II), Zn(II), Cu(II) and Cd(II) from aqueous solutions by adsorption onto olive branches activated carbon: Equilibrium and thermodynamic studies. Chemistry International 6(1) (2020) 11-20.

Mohan, D., Sarswat, A., Ok, Y.S., & Pittman Jr, C.U. (2014). Organic and inorganic contaminants removal from water with biochar, a renewable, low cost and sustainable adsorbent–a critical review. Bioresource Technology, 160, 191-202.

Muhammad, U. L., Zango, Z. U., & Kadir, H. A. 2019. Crystal violet removal from aqueous solution using corn stalk biosorbent. Science World Journal, 14(1), 133-138.

Needleman, H. (2004). Lead poisoning. Annual Review of Medicine, 55, 209-222.

Reddy, D.H.K., & Lee, S.M. (2013). Magnetic nanoparticle-based heavy metal removal: a review of the efficiency and regeneration aspects. Environmental Science: Processes & Impacts, 15(8), 1468-1487.

Shabelskaya, N., Egorova, M., Radjabov, A., Burachevskaya, M., Lobzenko, I., Minkina, T., & Sushkova, S. (2023). Formation of biochar nanocomposite materials based on $CoFe_2O_4$ for purification of aqueous solutions from chromium (VI). Water, 15(93).

Sonja, J., Ksenija, K., Danica, B.B., Bostjan, J., Matjaz, S., Tatjanai, T.P., Danilo, S.,

2019. Cobalt ferrite nanospheres as a potential magnetic adsorbent for chromium(VI) ions. J. Nanosci. Nanotechnol. 19(8), 5027e5034.

Tchounwou, P.B., Yedjou, C.G., Patlolla, A.K., & Sutton, D.J. (2012). Heavy metal toxicity and the environment. Experientia Supplementum, 101, 133-164.

UNICEF & WHO. (2019). Progress on household drinking water, sanitation and hygiene 2000-2017: Special focus on inequalities. New York: United Nations Children's Fund (UNICEF) and World Health Organization (WHO).

WHO. (2022). Guidelines for drinking-water quality: fourth edition incorporating the first addendum. Geneva: World Health Organization.

Yahya, N., Kashif, M., Nasir, N., Niaz Akhtar, M., Yusof, N.M., 2012. Cobalt ferrite nanoparticles: An innovative approach for enhanced oil recovery application. J. Nano Res. 17, 115e126. https://doi.org/10.4028/ www.scientific.net/JNanoR.17.115.

Zhang, G., Qu, J., Liu, H., Cooper, A.T., & Wu, R. (2010). $CuFe_2O_4$/activated carbon composite: A novel and effective catalyst for heterogeneous photo-Fenton decolorization of Orange II. Applied Catalysis B: Environmental, 99(1-2), 294-302. (Note: Example for magnetic AC composites, specific $CoFe_2O_3$ and SSHAC refs needed for actual dissertation).

Zhang, W., Duo, H., Li, S., An, Y., Chen, Z., Liu, Z., ... & Wang, X. (2020). An overview of the recent advances in functionalization biomass adsorbents for toxic metals removal. Colloid and Interface Science Communications, 38, 100308.